Journal of Cerebral Blood Flow & Metabolism (2015) 35, 1871–1881

www.jcbfm.com

ORIGINAL ARTICLE

Pharmacologically-induced neurovascular uncoupling is associated with cognitive impairment in mice

Stefano Tarantini[1,2,7], Peter Hertelendy[1,3,7], Zsuzsanna Tucsek[1], M Noa Valcarcel-Ares[1], Nataliya Smith[4], Akos Menyhart[3], Eszter Farkas[3], Erik L Hodges[1], Rheal Towner[4], Ferenc Deak[1,2], William E Sonntag[1,5], Anna Csiszar[1,2,5,6], Zoltan Ungvari[1,2,5,6] and Peter Toth[1,6]

There is increasing evidence that vascular risk factors, including aging, hypertension, diabetes mellitus, and obesity, promote cognitive impairment; however, the underlying mechanisms remain obscure. Cerebral blood flow (CBF) is adjusted to neuronal activity via neurovascular coupling (NVC) and this mechanism is known to be impaired in the aforementioned pathophysiologic conditions. To establish a direct relationship between impaired NVC and cognitive decline, we induced neurovascular uncoupling pharmacologically in mice by inhibiting the synthesis of vasodilator mediators involved in NVC. Treatment of mice with the epoxygenase inhibitor *N*-(methylsulfonyl)-2-(2-propynyloxy)-benzenehexanamide (MSPPOH), the NO synthase inhibitor L-NG-Nitroarginine methyl ester (L-NAME), and the COX inhibitor indomethacin decreased NVC by over 60% mimicking the aging phenotype, which was associated with significantly impaired spatial working memory (Y-maze), recognition memory (Novel object recognition), and impairment in motor coordination (Rotarod). Blood pressure (tail cuff) and basal cerebral perfusion (arterial spin labeling perfusion MRI) were unaffected. Thus, selective experimental disruption of NVC is associated with significant impairment of cognitive and sensorimotor function, recapitulating neurologic symptoms and signs observed in brain aging and pathophysiologic conditions associated with accelerated cerebromicrovascular aging.

Journal of Cerebral Blood Flow & Metabolism (2015) **35,** 1871–1881; doi:10.1038/jcbfm.2015.162; published online 15 July 2015

Keywords: behavior (rodent); cerebral hemodynamics; microcirculation; neurovascular coupling; EET; HETE; nitric oxide

INTRODUCTION

Cognitive impairment in the rapidly aging population poses a serious challenge to the western world. As the percent of the population over the age of 65 continues to increase, understanding potentially reversible and preventable vascular contributions to age-related dementia is of critical importance.

There is evidence that in addition to pathologies affecting the larger cerebral arteries (e.g., atherosclerosis leading to cerebral ischemia), pathophysiologic alterations of the cerebral microcirculation also have a critical role in the age-related decline of brain function.[1] Among them functional changes in the neurovascular unit affecting local regulation of cerebral blood flow (CBF) are of special importance. The energetic demand of neurons is high and the brain has little reserve capacity. With increased neuronal activity there is a requirement for rapid increases in oxygen and glucose delivery. This is regulated by neurovascular coupling (NVC), a feed-forward control mechanism adjusting local CBF to the energy requirements of activated neurons.[2] The resulting functional hyperemia is responsible for increased delivery of oxygen and glucose, effective elimination of noxious substances and ensuring an optimal microenvironment in the cerebral tissue. Neurovascular coupling is achieved through an orchestrated, tightly controlled intercellular communication between activated neurons and astrocytes and vascular endothelial cells, pericytes and smooth muscle cells.[2] The cellular mechanisms underlying NVC include neuronal and endothelial production of nitric oxide (NO)[3–5] and astrocytic production of vasodilator metabolites of arachidonic acid, including epoxygenase-derived epoxyeicosatrienoic acids (EETs) and cyclooxygenase-derived prostaglandins.[6–8]

Impairment of functional hyperemia ('neurovascular uncoupling') due to dysregulated production and/or release of NO, EETs, and prostaglandins is manifested in aging[9–11] and has also been described in a wide spectrum of pathophysiologic conditions associated with accelerated cerebromicrovascular aging and cognitive impairment, including hypertension,[12] obesity,[13] and Alzheimer's disease[14] both in humans and in experimental animals. Despite these advances, the relationship between neurovascular

[1]Donald W. Reynolds Department of Geriatric Medicine, Reynolds Oklahoma Center on Aging, University of Oklahoma Health Sciences Center, Oklahoma City, Oklahoma, USA; [2]Department of Physiology, University of Oklahoma Health Sciences Center, Oklahoma City, Oklahoma, USA; [3]Department of Medical Physics and Informatics, Faculty of Medicine and Faculty of Science and Informatics, University of Szeged, Szeged, Hungary; [4]Oklahoma Medical Research Foundation, Department of Pathology, Advanced Magnetic Resonance Center, Oklahoma City, Oklahoma, USA; [5]The Peggy and Charles Stephenson Cancer Center, University of Oklahoma Health Sciences Center, Oklahoma City, Oklahoma, USA and [6]Department of Neurosurgery, Szentagothai Research Center, University of Pecs, Pecs, Hungary. Correspondence: Dr Z Ungvari, Department of Geriatric Medicine, Reynolds Oklahoma Center on Aging, University of Oklahoma HSC, 975 N. E. 10th Street—BRC 1303, Oklahoma City, Oklahoma 73104, USA.
E-mail: zoltan-ungvari@ouhsc.edu
This work was supported by grants from the American Heart Association (ST, PT, AC, ZT, and ZU), the Oklahoma Center for the Advancement of Science and Technology (to FD, AC, ZU, and WES), the Oklahoma IDeA Network for Biomedical Research Excellence (to AC), the NIH (AG031085 to AC; AT006526 to ZU; AG038747 and NS056218 to WES), the Ellison Medical Foundation (to WES) and the Arkansas Claude Pepper Older Americans Independence Center at University of Arkansas Medical Center (to ZU; P30 AG028718).
[7]These authors contributed equally to this work.
Received 7 January 2015; revised 23 May 2015; accepted 29 May 2015; published online 15 July 2015

uncoupling and cognitive impairment is not completely understood.

Although impaired delivery of nutrients and oxygen is expected to adversely affect neuronal function, both aging and the aforementioned disease conditions are also associated with complex functional and phenotypic alterations both in neurons and in glial cells (including synaptic dysfunction, dysregulation of neurotransmitter receptors, and post-synaptic signaling pathways, impaired cellular metabolism, increased neuroinflammation, and neurodegenerative consequences of amyloid plaques), which exert multifaceted adverse effects on processes involved in higher cortical function.[15] Thus, in previous investigations it has been challenging to establish the specific role of neurovascular uncoupling in the genesis of cognitive impairment.

The present study was designed to test the hypothesis that neurovascular uncoupling itself, in the absence of primary neuronal deficit, results in clinically significant alterations of cerebral function, including cognitive impairment. To achieve this goal, neurovascular uncoupling was induced experimentally in healthy young control mice by treatment with specific pharmacological inhibitors of synthesis of NO, EETs, and prostaglandins followed by behavioral studies indicative for learning and memory, sensorimotor function, and gait coordination.

MATERIALS AND METHODS

All procedures were approved by the Institutional Animal Care and Use Committee of the University of Oklahoma Health Sciences Center and were reported in accordance with the ARRIVE guidelines.

Animals and Pharmacological Treatments

Male C57BL/6J mice (5 months old, $n = 120$) were purchased from the Jackson Laboratories (Bar Harbor, ME, USA). Animals were housed under specific pathogen-free barrier conditions in the Rodent Barrier Facility at University of Oklahoma Health Sciences Center under a controlled photoperiod (12 hours light; 12 hours dark). The animals were assigned into two groups: (1) animals with experimentally-induced neurovascular uncoupling receiving pharmacological inhibitors to disrupt production of mediators involved in functional hyperemia (NO, EETs, and prostaglandins) and (2) controls receiving vehicle. To inhibit the production of EETs, mice were treated with *N*-(methylsulfonyl)-2-(2-propynyloxy)-benzenehexanamide (MSPPOH), a specific inhibitor of EET-producing epoxidases.[16] Alzet osmotic minipumps (7 days-1 μL/h, ~200 μL total volume, Cat No.: 2001; Durect Corp., Cupertino, CA, USA) were filled with MSPPOH (20 mg/kg per day, dissolved in DMSO and diluted to final concentration with 45% cyclodextrin[16]) and implanted subcutaneously. Sham-operated control animals received vehicle. To block production of vasodilator NO, mice were treated with the NO synthase inhibitor L-NG-Nitroarginine methyl ester (L-NAME, 100 mg/kg per day; in drinking water).[17] Indomethacin (INDO; 7.5 mg/kg per day, p.o.), a nonselective inhibitor of cyclooxygenases, was used to disrupt NVC by cyxlooxygenase-derived vasodilator arachidonic acid metabolites. Indomethacin was dissolved in ethanol and diluted in 5% (w/v) sodium bicarbonate solution. The maximum administered daily volume of ethanol was 3 μL per animal. The treatments were continued throughout the entire experimental period (7 days). Blood pressure of the animals was recorded before the treatment and on day 3 of the treatment period by the tail cuff method, as described.[18]

Behavioral Studies

After the animals completely recovered from surgery (day 3) behavioral tasks were performed to characterize the effect of pharmacologically-induced neurovascular uncoupling on learning and memory, sensorymotor function, gait and locomotion ($n = 20$ in each group).

Spatial memory testing of mice in the Y-maze. Animals were tested for spatial working memory in the Y-maze. In brief, a Y-maze apparatus, made up of three enclosed transparent Plexiglas arms (40 cm length × 9 cm width × 16 cm height) with extra-maze visual cues around the maze, was used to assess hippocampal-dependent spatial recognition memory. The test consisted of two trials separated by an intertrial interval (4 hours). All mice were transported to the behavioral testing room in their home cages at least 1 hour before testing. In the first training (acquisition) trial, mice were placed in the maze facing the end of a pseudorandomly chosen start arm and allowed to explore the maze for 5 minutes with one of the arms closed (novel arm). Mice were returned to their home cage until the second (retrieval) trial, during which they could explore freely all three arms of the maze. The time spent in each arm and the number of entries were measured and analyzed from video recordings (Ethovision, Noldus Information Technology Inc., Leesburg, VA, USA). Mice were required to enter an arm with all four paws in order for it to be counted as an entry. Entering the Novel arm more frequently and for longer periods of time indicates intact memory and novelty-seeking behavior because of the innate tendency of mice to explore. The maze was cleaned with 70% ethanol between the trials.

Novel object recognition test. To evaluate recognition memory, the novel object recognition task was used. The results of the test are influenced by both hippocampal and cortical impairment.[19] The test consists of a habituation phase, acquisition (familiarization) phase, and trial phase. During the habituation phase, the animals explored the empty open-field arena for 5 minutes. Then, in the acquisition phase the mice explore two identical objects for 2 minutes. After a 4-hour delay, a trial phase occurred. During this period, animals explored the familiar object and a novel object for 2 minutes. Exploration of the objects was defined as directing the nose at a distance of $\leqslant 2$ cm to the object and/or touching it with the nose. Sitting or climbing on it was not considered as an exploration. All objects used in this study were made of washable odorless plastic and were different in shapes and colors but identical in size. A percent of time spent exploring the novel object relative to the total time spent exploring both objects was used as a measure of novel object recognition. The recognition index (RI, representing the time spent investigating the novel object [T_{novel}] relative to the total object investigation) was used as the main index of retention, which was calculated according to the following formula: $[RI = T_{novel}/(T_{novel}+T_{familiar})]$.[19] The arena and the objects were cleaned with 70% ethanol between the trials to prevent the existence of olfactory cues.

Elevated plus maze learning protocol. Mice were also assessed for learning capacity using an elevated plus maze-based learning protocol as previously described.[18] A gray elevated plus maze was used. Two open arms (25 × 5 cm) and two (25 × 5 cm) closed arms were attached at right angles to a central platform (5 × 5 cm) 40 cm above the floor. Mice were placed individually at the end of an open arm with their back to the central platform. The time for mice to cross a line halfway along one of the closed arms was measured (transfer latency) on the first day and the second day. Mice had to have their body and each paw on the other side of the line. If a mouse had not crossed the line after 120 seconds, then it was placed beyond it. After crossing the line, mice had 30 seconds to explore the apparatus. Learning was defined as reduced transfer latency on day 2 compared with day 1. Decreased transfer latency indicates intact hippocampal function.

Rotarod. Motor coordination was assessed in control and treated mice by using an automated four-lane rotarod (Columbus Instruments, Columbus, OH, USA). Mice were pretrained by placing them on the moving rotarod at 10 r.p.m. until they performed at this speed for 120 seconds. On the day of testing, mice were habituated in their home cages and acclimate to the testing room for at least 15 minutes. The test phase consisted of three trials separated by 15 minutes intertrial intervals. The testing apparatus was set to accelerate from 4 to 40 r.p.m. in 300 seconds. One mouse was then placed on each lane and the rotarod was started with an initial rotation of 4 r.p.m. The rotational velocity was set to increase every 10 seconds and the latency to fall was recorded. Latency to fall was recorded in seconds by an infra-red beam across the fall path along with the max r.p.m. sustained by each mouse.[20]

Grip strength. To evaluate the effect of neurovascular uncoupling on static force production, forelimb grip strength was measured using a computerized electronic pull strain gauge (Grip Strength Meter-Columbus Instruments, Columbus, OH, USA).

Adhesive removal test. Sensorimotor function was characterized by the adhesive removal test.[21] This test consists of applying adhesive tape on each forepaw of the animal and measuring the time-to-remove. In brief, mice were individually habituated for 20 minutes to a test cage with clean bedding. The animals were then removed from the testing box and a

precut square piece of tape was applied on each animal front paw to cover the hairless part of the forepaws. After the adhesive squares were placed with equal pressure on each forepaw, the animals were replaced in the testing box and the latency for the mice to remove the pieces of tape was measured with a maximum test time of 120 seconds.

Buried food retrieval test. To evaluate the effect of neurovascular uncoupling on olfactory ability and gustatory motivation, we used the buried food retrieval test. Mice deprived of food overnight were put in a cage ($42 \times 25 \times 15\ cm^2$) in which a food pellet was buried under bedding material and the latency to discover it was measured with a maximum of 5 minutes. The same test was repeated after 1 hour with a food pellet in a visible position in front of the mouse to exclude motor deficits or motivational failure.

Analysis of gait function. To determine whether neurovascular uncoupling affects gait coordination, we tested the animals using an automated computer assisted method (CatWalk; Noldus Information Technology Inc.). Using the CatWalk system, the detection of paw print size, pressure, and pattern during volunteer running on an illuminated glass walkway by a camera placed under the glass surface provides an automated analysis of gait function and the spatial and temporal aspects of interlimb coordination.[22] Briefly, animals were trained to cross the walkway and then, in a dark room and silent room (< 20 lux of illumination), animals were tested in three consecutive runs. Data were averaged across three runs in which the animal maintained a constant speed across the walkway. After manual identification and labeling of each footprint, the following indices were calculated. The regularity index (%) is a fractional measure of interpaw coordination, which expresses the number of normal step sequence patterns relative to the total number of paw placements. The formula of regularity index is $NSSP \times 4/PP \times 100$ (%), where NSSP represents the number of normal step sequence patterns and PP the total number of paw placements. In healthy, fully coordinated animals its value is 100%. Phase dispersion provides a quantitative metric of interpaw coordination. Phase dispersion characterizes the placement of two paws ('target' and 'anchor') during the cycle of consecutive initial contacts with an 'anchor' paw. In a step cycle base of support gives the distance between the mass midpoints of the fore prints at maximal contact. The results are averaged and expressed in cm.

Measurement of Neurovascular Coupling Responses and Somatosensory Evoked Field Potentials

After behavioral testing, mice in each group were anesthetized (α-chloralose (50 mg/kg, intraperitoneally)/urethane (750 mg/kg, intraperitoneally), endotracheally intubated and ventilated (MousVent G500; Kent Scientific Co, Torrington, CT, USA). A thermostatic heating pad (Kent Scientific Co) was used to maintain the rectal temperature at 37°C.[23] End-tidal CO_2 (including dead space) was controlled between 3.2% and 3.7% to keep blood gas values within the physiologic range ($PaCO_2$: 37.1 ± 2.4 mm Hg, PaO_2: 110.8 ± 3.5 mm Hg). The right femoral artery was canulated for arterial blood pressure measurement (Living Systems Instrumentations, Burlington, VT, USA).[23] The blood pressure was within the physiologic range throughout the experiments (90 to 110 mm Hg). Mice were immobilized, placed on a stereotaxic frame (Leica Microsystems Inc, Buffalo Grove, IL, USA), the scalp and the periosteum were pulled aside. The animals were equipped with an open cranial window as described[23] and a glass-insulated tungsten microelectrode (impedance, 2 to 3 MΩ, Kation Scientific, LLC, Minneapolis, MN, USA) was inserted stereotaxically into the left barrel cortex (3 mm lateral and 1.5 mm caudal to bregma; depth of 0.6 mm) through the artificial cerebrospinal fluid-perfused open cranial window for recording local field potentials. An Ag/AgCl electrode inserted in the neck muscles served as a reference electrode. Changes in CBF were assessed above the left barrel cortex using a laser Doppler probe (Transonic Systems Inc., Ithaca, NY, USA) as described.[23]

After basal activity was recorded the right whisker pad was stimulated by a bipolar stimulating electrode placed to the ramus infraorbitalis of the trigeminal nerve and into the masticatory muscles. The stimulation protocol used to investigate NVC and somatosensory evoked field potentials consisted of 10 stimulation presentation trials with an intertrial interval of 70 seconds, each delivering a 30-second train of electrical pulses (2 Hz, 0.2 mA, intensity, and 0.3 ms pulse width) to the mystacial pad after a 10-second prestimulation baseline period. Changes in CBF were averaged and expressed as percent (%) increase from the baseline value.[12] The electrical signal was amplified with a AC/DC differential amplifier (high pass at 1 Hz, low pass at 1 kHz) (Model 3000, A-M Systems, Inc., Carlsborg, WA, USA), and digitalized by the PowerLab/Labchart data acquisition system (ADInstruments, Colorado Springs, CO, USA) with the sampling rate of 40 kHz. Analyses were performed on the average of 10 stimulation trials. The negative amplitude in the somatosensory evoked field potential response was considered as the excitatory postsynaptic potential (fEPSP).[24] Experiments lasted ~20 to 30 minutes/mouse, which permitted stable physiologic parameters to be obtained. The experimenter was blinded to the treatment of the animals. In additional experiments, the effects of acute topical treatment with MSPPOH (2×10^{-6} mol/L for 30 minutes), L-NAME (3×10^{-4} mol/L), and indomethacin (10^{-5} mol/L for 30 minutes) on NVC in untreated mice was assessed.

Measurement of Changes in Extracellular Glucose Concentration in Response to Whisker Stimulation

In a separate cohort of animals, we assessed changes in extracellular glucose concentration ($[glucose]_{ec}$) in response to whisker stimulation, as a metabolic surrogate of cerebral functional hyperemia. Glucose and lactate produced from glucose are the primary source of energy of cerebral tissue.[25] Because there are no significant glucose reserves, NVC has a critical role in increasing glucose supply during neuronal and astrocytic activation in a feed-forward manner. Thus, measurement of changes in $[glucose]_{ec}$ during neuronal activation, which is determined by the balance between cellular consumption and changes in CBF, can be used as a metabolic surrogate of cerebral functional hyperemia. In brief, a cranial window was prepared in anesthetized mice and the dura was gently removed. The cranial window was superfused continuously with artificial cerebrospinal fluid. Glucose microsensors with constant potential amperometry were used to measure changes of extracellular glucose concentration in response to whisker stimulation. A 3-electrode potentiostat (Quadstat) with an eDAQ data acquisition system (eDAQ Pty Ltd., Colorado Springs, CO, USA) was used. Before placing the glucose sensor (Sarissa GLU Biosensor, 25 μm tip, Sarissa Biomedical, Coventry, UK)[26] into the barrel field of the mouse, it was calibrated according to the manufacturer guidelines *in vitro*, then inserted 1.5 mm caudal and 3 mm lateral from bregma into the cerebral tissue approximately 500 μm deep. The glucose sensor is a platinum/iridium wire electrode encapsulated in a bio-layer containing glucose oxidase and protected against the interference with ascorbate, urate, dopamine, and 5-hydroxytriptamine. D-Glucose is oxidized into D-glucono-1,5-lactone plus hydrogen peroxide, which is sensed by the electrode. In a different set of experiments, glucose null sensors (lack of any enzymes for biosensing) were used as controls. The reference electrode (Ag/AgCl) was placed in the cerebral tissue elsewhere and the auxiliary electrode (Ag/AgCl) was between the scalp and the skull. Constant potential 0.5 V versus Ag/AgCl was used. After the insertion a stable baseline developed in 5 to 10 minutes. Then, the right whiskers were stimulated for 2 minutes at 5 Hz in two consecutive trials divided by 5 to 10 minutes intervals. The response was recorded in μA and converted to mmol/L of glucose using the calibration curve.

Arterial Spin Labeling Magnetic Resonance Imaging

To characterize the effect of the drugs used to inhibit NVC on basal CBF, a separate cohort of control and experimental mice ($n = 10$ in each group) were positioned in a stereotaxic cradle for perfusion MRI studies. The animals were anesthetized with isoflurane administered through a face-mask and adjusted to maintain respiratory rate in the physiologic range following published protocols.[27] Body temperature was maintained at ~37°C using a heading pad. A 30-cm horizontal bore Bruker Biospin magnet operating at 7 T (Bruker BioSpin GmbH, Karlsruhe, Germany) was used with a S116 gradient set. An actively decoupled head coil was used for signal detection. The resonator coil was a multirung birdcage quadrature coil with an inner diameter of 72 mm. Multiple-slice, multiple echo imaging ($T_R = 2{,}000$ ms, $T_E = 17.5$ or 58.2 ms, 156 μm/pixel, 2 averages) was used to obtain gross brain morphology. Perfusion maps were obtained on a single axial slice of the brain located 1.5 mm posterior from bregma on the rostro-caudal axis. The imaging geometry was a $25.6 \times 25.6\ mm^2$ slice of 1.5 mm in thickness, with a single shot echo-planar encoding over a 64×64 matrix. An echo time of 20 ms and a repetition time of 18 seconds were used, and images were not submitted to time averaging. To obtain perfusion contrast, the flow alternating inversion recovery scheme was used. Briefly, inversion recovery images were acquired using a slice-selective (SS) inversion of the same geometry as the imaging slice or a nonselective (NS) inversion slice concentric with the imaging slice but of

60 mm in thickness. For each type of inversion, eight images were acquired with inversion times (TI) evenly spaced from 20 ms to 2,820 ms.

Data processing. Recovery curves were obtained as previously reported,[28] and obtained from each pixel of the NS ($S_{NS}(TI) = A - B \times e^{-TI/T1}$) or selective ($S_{ss}(TI) = A - B \times e^{-TI/T1^*}$, with $1/T_1^* = 1/T_1 + CBF/\lambda$) inversion images were numerically fitted to derive the pixelwise T_1 and T_1* values, respectively. The results were stored as maps for further analysis. These longitudinal recovery rates were then used to calculate the perfusion by CBF (mL/(100 g min)) on a pixelwise basis using the following relationship: $CBF = \lambda \times [(1/T_1^*) - (1/T_1)]$. The perfusion was scaled by assigning the generally adopted value of 0.9 mL/g[29] to the partition coefficient, λ. Regions of interest were manually outlined around the left and right cortex regions of the brain.

Electrophysiologic Studies: Measurement of Long-Term Potentiation

To determine whether the pharmacological treatment disrupted neuronal mechanisms of learning and memory, extracellular recordings were performed from acute hippocampal slices with an adopted protocol as originally described.[30] Briefly, horizontal hippocampal slices of 325 μm thickness from mice in each cohort were prepared in ice-cold solution containing (in mmol/L) sucrose 110, NaCl 60, KCl 3, NaH_2PO_4 1.25, $NaHCO_3$ 28, sodium ascorbate acid 0.6, glucose 5, $MgCl_2$ 7, $CaCl_2$ 0.5 using a HM650V vibrating microtome (Thermo Scientific, Burlington, ON, USA). Slices were then transferred to a holding chamber (Scientific Designs, Inc., Little Ferry, NJ, USA), which contained oxygenated artificial cerebrospinal fluid of the following composition (in mmol/L) NaCl 126, KCl 2.5, NaH_2PO_4 1.25, $MgCl_2$ 2, $CaCl_2$ 2, $NaHCO_3$ 26, glucose 10, pyruvic acid 2, ascorbic acid 0.4. For *in vitro* inhibition of synthesis of NO, EETs and prostaglandins MSPPOH (2×10^{-6} mol/L for 30 minutes), L-NAME (3×10^{-4} mol/L), and indomethacin (10^{-5} mol/L for 30 minutes) were used. Slices were left to recover for at least 60 minutes at room temperature before recording in a brain slice chamber (Automate Scientific Inc., Berkeley, CA, USA). Slices from the treatment and control groups were positioned on P5002A multi-electrode arrays (Alpha MED Scientific Inc., Saito-asagi, Ibaraki, Osaka, Japan) and perfused with artificial cerebrospinal fluid at a rate of 2 mL/min, equilibrated with 95% O_2 and 5% CO_2 at 32°C. Field excitatory postsynaptic potentials were invoked through stimulation of the performant path collaterals (0.2 msec biphasic pulse) and obtained from the dentate gyrus area. Threshold for evoking fEPSPs was determined and the stimulus was increased incrementally until the maximum amplitude of the fEPSP was reached (I/O curve). All other stimulation paradigms were induced at the same half-maximal stimulus strength, defined as 50% of the stimulus used to produce the maximum fEPSP amplitude, as determined by the I/O curve, for each individual slice. After a stable baseline recording of 15 minutes was established, long-term potentiation was induced using high-frequency stimulation, which consisted of 100 pulses at 100 Hz applied 4 times with half-minute intervals. Field excitatory postsynaptic potentials were monitored every 30 seconds for 60 minutes after high-frequency stimulation and were recorded with MED-64 system and Mobius software (Alpha MED Scientific Inc). Potentiation was calculated as the percent increase of the mean fEPSP descending slope after high-frequency stimulation and normalized to the mean fEPSP descending slope of baseline recordings.

Statistical Analysis

Statistical analysis was performed by unpaired *t* test or two-way ANOVA for repeated measures followed by Bonferroni multiple comparison test, as appropriate, using Prism 5.0 for Windows (Graphpad Software, La Jolla, CA, USA). A *P* value of less than 0.05 was considered as statistically significant. Data are expressed as mean ± s.e.m. Sample size was based on expected variances and differences between groups.

RESULTS

Pharmacologically-Induced Neurovascular Uncoupling

Changes in CBF in the whisker barrel cortex in response to contralateral whisker stimulation were significantly decreased by *in vivo* treatment with MSPPOH+NAME+INDO (representative tracings are shown in Figure 1A and summary data are shown in Figure 1B).[31] We found that acute topical treatment with MSPPOH+NAME+INDO also results in similar decreases in the NVC response (Figure 1B). Treatment with MSPPOH+NAME+INDO did not affect relative baseline CBF measured by laser Doppler flowmetry ($P = 0.73$ MSPPOH+NAME+INDO versus pretreatment baseline). We also measured changes in $[glucose]_{ec}$ during neuronal activation, as a metabolic surrogate of cerebral functional hyperemia. We found that $[glucose]_{ec}$ increased in the barrel field of the somatosensory cortex during contralateral whisker stimulation in control animals, corresponding to the dynamics of the CBF response (Figures 1B and 1C). In contrast, the glucose response associated with neuronal activation was blunted in animals treated with MSPPOH+NAME+INDO ($P = 0.002$ versus control; Figures 1B and 1C).

Pharmacological treatments could reduce functional hyperemia by impairing neural activity evoked by whisker pad stimulation. To examine this possibility, we assessed the effects of treatment with MSPPOH+NAME+INDO by recording spontaneous and evoked neural activity. We found that the amplitude and frequency distribution of the electrocorticogram and the amplitude of the somatosensory field potentials produced by activation of the whisker pad do not differ between control and chronically MSPPOH+NAME+INDO treated mice and are also unaffected by acute administration of MSPPOH+NAME+INDO into the cranial window (Figures 1E and 1F). Therefore, treatment with MSPPOH

Figure 1. Experimentally induced neurovascular uncoupling in mice. (**A**) Representative traces of cerebral blood flow (CBF) measured with a laser Doppler probe above the whisker barrel cortex during electrical stimulation of the contralateral whisker pad (current: 0.2 mA, pulse duration: 0.3 ms, at 2 Hz for a 30-second period) before (left) and after (middle) topical administration of *N*-(methylsulfonyl)-2-(2-propynyloxy)-benzenehexanamide (MSPPOH), L-NG-Nitroarginine methyl ester (L-NAME) plus indomethacin (INDO; see Materials and methods) through the cranial window. Right: representative trace of CBF response obtained in a mouse treated chronically with MSPPOH, L-NAME plus INDO (see Materials and methods). (**B**) Bar graphs depict the summary data of the effect of MSPPOH+NAME+INDO treatment on CBF responses to whisker stimulation. Data are mean ± s.e.m. (control: $n = 9$, treated: $n = 6$, $^*P < 0.01$ versus Control). (**C**) Original recordings of changes in extracellular glucose ($[glucose]_{ec}$) in response to whisker stimulation (5 Hz, 2 minutes) measured by amperometry using a glucose biosensor inserted into the barrel cortex of mice treated with MSPPOH+NAME+INDO or vehicle. '0 sensor': signal obtained with a biosensor constructed the same way as the glucose sensors, without the enzymes necessary for biosensing. Summary data are shown in (**D**). In animals treated with MSPPOH+NAME+INDO the glucose response elicited by whisker stimulation was significantly decreased. Data are mean ± s.e.m. ($n = 6$ in each group, $^*P = 0.002$ versus Control). (**E**) Representative recordings showing the effect of treatment with MSPPOH+NAME+INDO on somatosensory evoked potential (SEP) responses in the primary somatosensory cortex in response to electrical stimulation of the contralateral whisker pad in control and treated groups. Amplitude peaks of SEP are labeled P1 and N1 to reflect their polarity and sequence. Inlet shows spontaneous cortical electric activity. (**F**) The amplitudes of the negative waves (N1) were unaffected by either acute administration of MSPPOH+NAME+INDO in the cranial window ($n = 6$, $P = 0.2$) or chronic treatment of the mice with MSPPOH+NAME+INDO (control: $n = 9$, treated: $n = 6$, $P = 0.4$). (**G**) T1-weighted morphological MRI scans and the corresponding perfusion map in the brain of a control and a MSPPOH+NAME+INDO treated mouse are shown. The slice is located 1 to 1.5 mm posterior from bregma, the yellow circles show regions of interest (ROIs) placed on the barrel field where cerebral blood flow (CBF, mL/100 g min) measurements were taken. Summary data for basal perfusion (mean ± s.d.; $n = 10$ in each group) are shown in (**H**) (n.s.: $P = 0.139$).

+NAME+INDO is unlikely to contribute to impaired functional hyperemia by modulating the neural activity evoked by whisker stimulation.

Pharmacologically-induced impairment of NVC responses was an isolated phenomenon, which does not appear to be associated with changes in systemic hemodynamic parameters. Accordingly,

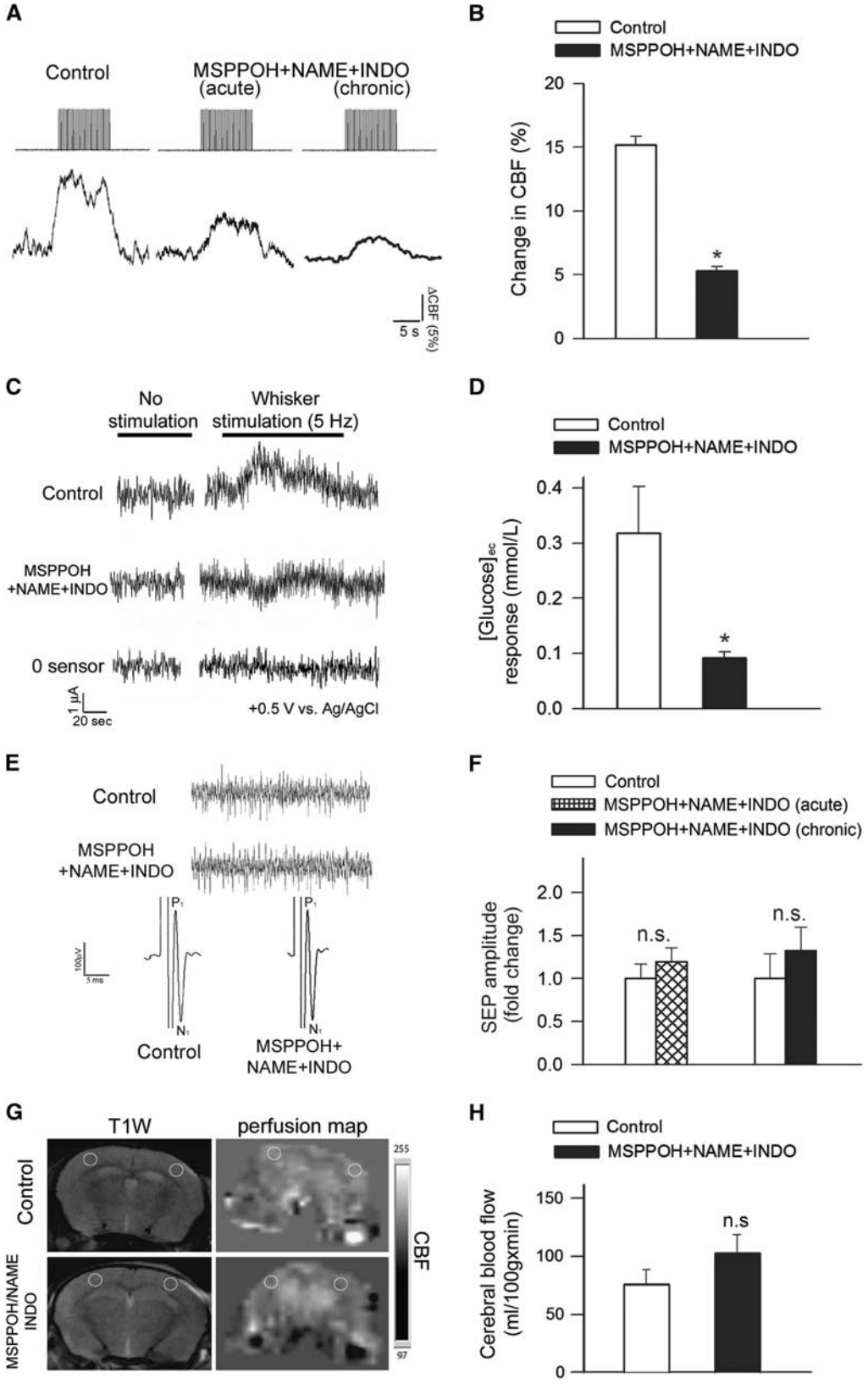

the blood pressure of the two groups of animals did not differ significantly (control: 106 ± 2 mm Hg; MSPPOH+NAME+INDO treated: 107 ± 3 mm Hg; $P = 0.49$). Further, perfusion mapping of cerebral coronal slices in each group of animals was performed by MRI 1 to 1.5 mm posterior from the bregma, which corresponds to the barrel field of the primary somatosensory cortex. We found that calculated CBF values did not differ between the control and MSPPOH+NAME+INDO groups ($P = 0.139$; Figures 1E and 1F).

Induction of Neurovascular Uncoupling Is Associated with Impaired Cognitive Function

For the hippocampus-dependent spatial memory test, control mice spent significantly ($P = 0.006$) more time in the novel arm than the previously visited arms after the intertrial interval. Mice treated with MSPPOH+NAME+INDO spent significantly less time in the novel arm (Figure 2B). Only the control mice entered the novel arm more often than the previously visited arms ($P = 0.001$ versus Other arm; Figure 2A), whereas mice treated with MSPPOH+NAME +INDO did not ($P = 0.36$ Novel arm versus Other arm), indicating that experimentally-induced neurovascular uncoupling leads to impaired spatial working memory and novelty-seeking behavior.

We also evaluated hippocampal-dependent learning and memory employing the elevated plus maze. For control mice, transfer latency on day 2 was significantly decreased (by ~37%; $P = 0.027$) compared with day 1 (Figure 2C), indicating an intact learning effect. In contrast, for mice treated with MSPPOH+NAME +INDO the transfer latency on day 1 and day 2 was similar ($P = 0.71$ first day versus secnd day), indicating impaired learning capability.

Subsequently, we also tested the performance of the mice in the novel object recognition test. We found no significant difference in the time that mice from each group spent exploring the two identical objects placed at the opposite ends of the arena during the acquisition phase, confirming that the location of the objects did not affect the exploration behavior of mice. In the trial phase with two different objects (one novel, the other familiar), control mice explored the novel object for a significantly longer time period, with a calculated RI of 70 ± 2.8%, indicating their memory for the familiar object (Figure 2D). In contrast, mice treated with MSPPOH+NAME+INDO had a lower RI at 59 ± 4% ($P = 0.03$). This result is consistent with their impaired hippocampal- and cortical-dependent recognition memory (Figure 2D).

Effects of Neurovascular Uncoupling on Sensorimotor Function and Gait Coordination

In addition to impaired spatial learning and memory sensorimotor deficits are the most common consequences of the aging process in the central nervous system both in humans and in laboratory animals. We found that mice treated with MSPPOH+NAME+INDO had impaired motor performance on Rotarod compared with control mice, as shown by a significant decrease in latency to fall ($P = 0.031$ versus Control) from the rotating lanes of the Rotarod and they also fell at lower velocity (r.p.m.) ($P = 0.021$ versus Control) (Figures 3A and 3B).

Static force production activates a network of sensorimotor cortical and subcortical regions, which is associated with increases in local CBF in humans.[32] Further, pathologic conditions, which lead to neurovascular uncoupling (e.g., obesity), are often associated with impaired grip strength in humans.[33] We found that static force production was also significantly decreased in mice treated with MSPPOH+NAME+INDO ($P = 0.01$ versus Control; Figure 3C).

To further evaluate sensory-motor function, we also performed the adhesive removal test. We found that although there was a trend for increased latency to remove the tactile stimulus from the paws (Figure 3D) in mice treated with MSPPOH+NAME+INDO, the difference did not reach statistical significance.

Despite the presence of significant odor-evoked functional hyperemia in mice[34] we found that the combined inhibition of synthesis of NO, prostaglandins, and EETs does not affect olfactory ability and gustatory motivation ($P = 0.4$ versus control; Figure 3E).

Gait coordination is a higher integrative process of the sensorimotor system. Clinical studies suggest that NVC may be involved in preservation of gait function in elderly people.[35] Yet, in the present study we did not observe differences between control mice and mice treated with MSPPOH+NAME+INDO in parameters indicative of gait (regularity index $P = 0.43$ versus control, Base of support $P = 0.32$ versus control, Phase dispersion LF-RF $P = 0.56$, LH-RH $P = 0.12$, LF-RH $P = 0.88$, RF-LH $P = 0.61$; Figures 3F–3K).

No Direct Changes in Synaptic Mechanisms of Hippocampal Learning and Memory

To determine whether treatment with MSPPOH+NAME+INDO directly affects major cellular mechanisms underlying learning and memory, we measured long-term potentiation in the dentate gyrus in hippocampal brain slice preparations after 4 × 100 Hz tetanic stimulation of the perforant pathway. The fEPSP slope increased similarly in control and MSPPOH+NAME+INDO treated groups ($P = 0.93$) during the 60-minute experimental period (Figure 4). To add further *ex vivo* data to the *in vivo* evoked field potential responses, we also measured fEPSP in the dentate gyrus to electrical stimulation of the perforant pathway (with 5 μA steps increased up to 100 μA). We found that the ratio of evoked responses to the presynaptic fiber volley was similar in both groups ($P = 0.78$), showing that the pharmacological treatment does not affect neuronal EPSP. Collectively, these results indicate that there are no significant differences in synaptic function and neuronal mechanisms of learning and memory between the two experimental groups.

DISCUSSION

This is the first study, to our knowledge, to show that pharmacologically-induced neurovascular uncoupling in mice is associated with cognitive impairment that mimic behavioral alterations present in mouse models of aging and age-related diseases.

Population-based studies show that vascular risk factors are associated with significantly elevated risk for late life cognitive decline.[36] Moreover, evidence exists that microvascular health is critical to delay the onset of vascular cognitive impairment.[36] Research to date suggests a complex interaction between vascular risk factors, cerebromicrovascular pathologies, and the pathogenesis of cognitive decline, in which neurovascular uncoupling likely have a critical role.

In the present study, we show that pharmacological inhibition of synthesis of EETs, prostaglandins, and NO leads to significant neurovascular uncoupling, characterized by intact evoked field responses that associate with impaired CBF responses induced by synaptic activity (Figure 1). This experimentally-induced neurovascular uncoupling mimics impairment of functional hyperemia observed in aging[23] and pathophysiologic conditions associated with accelerated cerebromicrovascular aging, including hypertension,[12] obesity,[13] and Alzheimer's disease.[14] The physiologic consequences of neurovascular uncoupling are likely multifaceted. Here, we show that neurovascular uncoupling is associated with impaired delivery of glucose to the activated brain region (Figure 1). Although the relatively modest changes in extracellular glucose levels are likely not directly related to impaired cortical function associated with neurovascular uncoupling, they serve as a metabolic surrogate of the impaired hyperemic response. On the basis of previous studies,[37,38] we

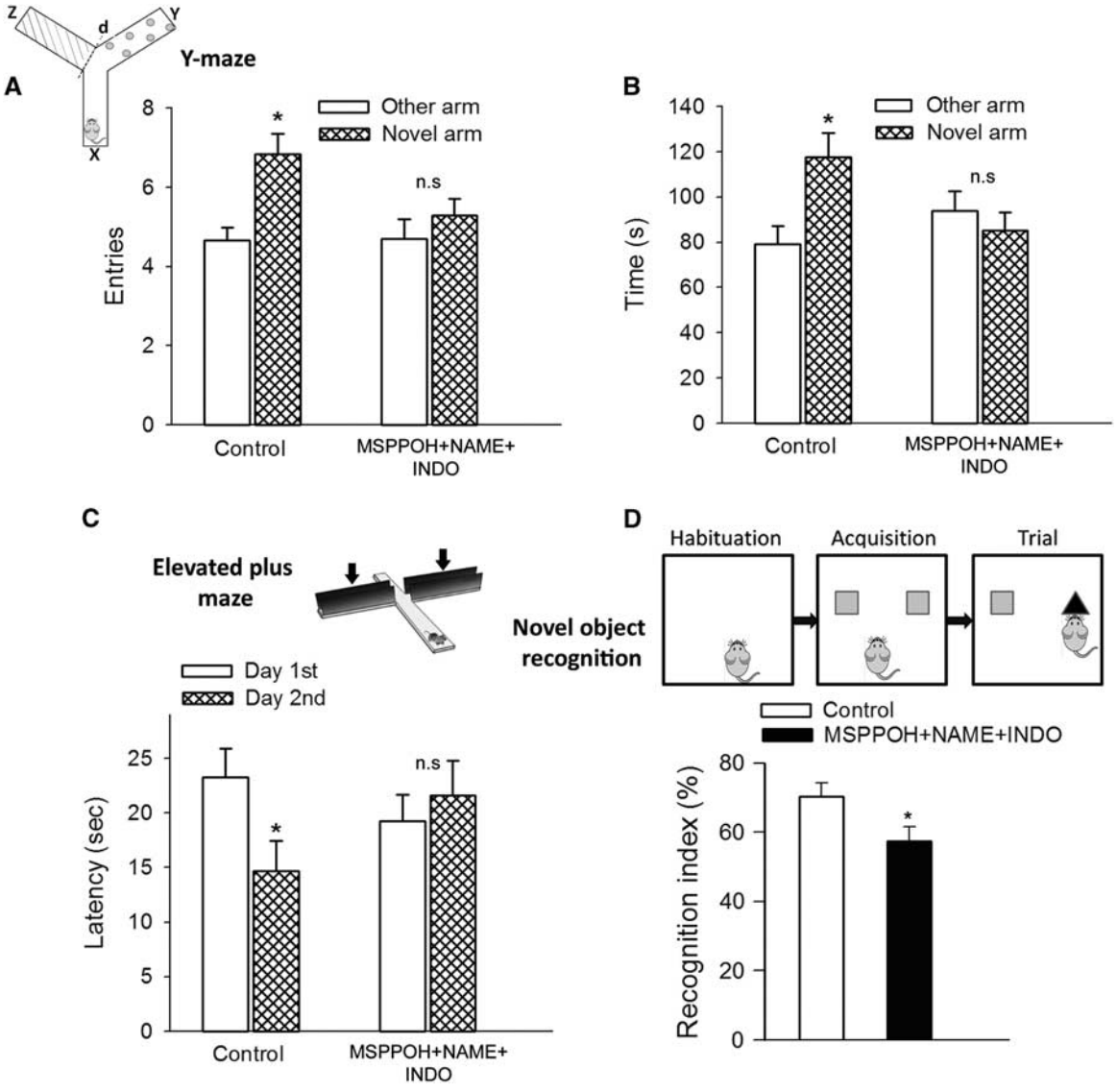

Figure 2. Neurovascular uncoupling impairs learning and memory. (**A** and **B**) Spatial memory testing of mice in Y-maze. The inset shows schematic picture of the Y-maze with extra-maze cues used for testing spatial memory (x: start arm, y: other arm, z: novel arm, see details in text). Number of entries in novel arm (**A**, $^*P = 0.006$ versus other arm in control mice) and exploratory time spent in novel arm of the Y-maze during retrieval trial (**B**, and $P = 0.001$ versus other arm in control mice) are shown. Mice treated with MSPPOH+NAME+INDO exhibited impaired spatial memory as shown by the similar number of entries ($P = 0.46$) and exploratory time ($P = 0.36$) spent in novel arm and the other arm of Y-maze during the retrieval trial. Data are mean ± s.e.m. ($n = 20$ in each group). (**C**) Neurovascular uncoupling impairs learning ability, as assessed using the elevated plus maze-based learning protocol (see Materials and methods for details). Control mice exhibited significantly decreased transfer latency on day 2 ($^*P = 0.027$ versus Day 1) indicating intact hippocampal-dependent learning. For mice treated with MSPPOH+NAME+INDO transfer latency was similar on days 1 and 2 ($P = 0.71$) indicating that these mice had significantly impaired learning ability. Data are mean ± s.e.m. ($n = 20$ in each group). (**D**) The novel object recognition task test is used to evaluate recognition memory in mice (inset). During the habituation phase, the animals explored the empty open-field arena for 5 minutes. Then, in the acquisition phase the mice explored two identical objects during 2 minutes. After a 4-hour delay, a trial phase occurred. The recognition index (representing the time spent investigating the novel object relative to the total object investigation) was used as the main index of retention. Data are mean ± s.e.m. ($n = 20$ in each group). $^*P < 0.05$ versus control. INDO, indomethacin; MSPPOH, *N*-(methylsulfonyl)-2-(2-propynyloxy)-benzenehexanamide; L-NAME, L-NG-Nitroarginine methyl ester.

predict that impaired NVC may result in impaired nutrient delivery, inadequate wash-out of by-products, and altered local microenvironment in the cerebral tissue, all of which may adversely affect neuronal function.

The present study provides evidence that neurovascular uncoupling is associated with cognitive impairment. This is complementary to previous data demonstrating that global reduction of basal CBF also leads to significant learning deficits.[39] We found that pharmacological inhibition of synthesis of EETs, prostaglandins, and NO associates with impaired performance in tests relevant for hippocampal- and/or cortical-dependent tasks of learning and memory (Figure 2), suggesting that neurovascular uncoupling predicts cognitive decline. Our findings have important clinical relevance. First, a wide range of pathophysiologic conditions were shown to adversely affect the synthesis of vasodilator NO, EETs, and prostaglandins, promoting neurovascular uncoupling. For example, several cardiovascular risk factors, including hypertension, dyslipidaemia, smoking, and obesity, which are important risk factors for cognitive decline in elderly patients,[36,40] were shown to decrease the bioavailability of

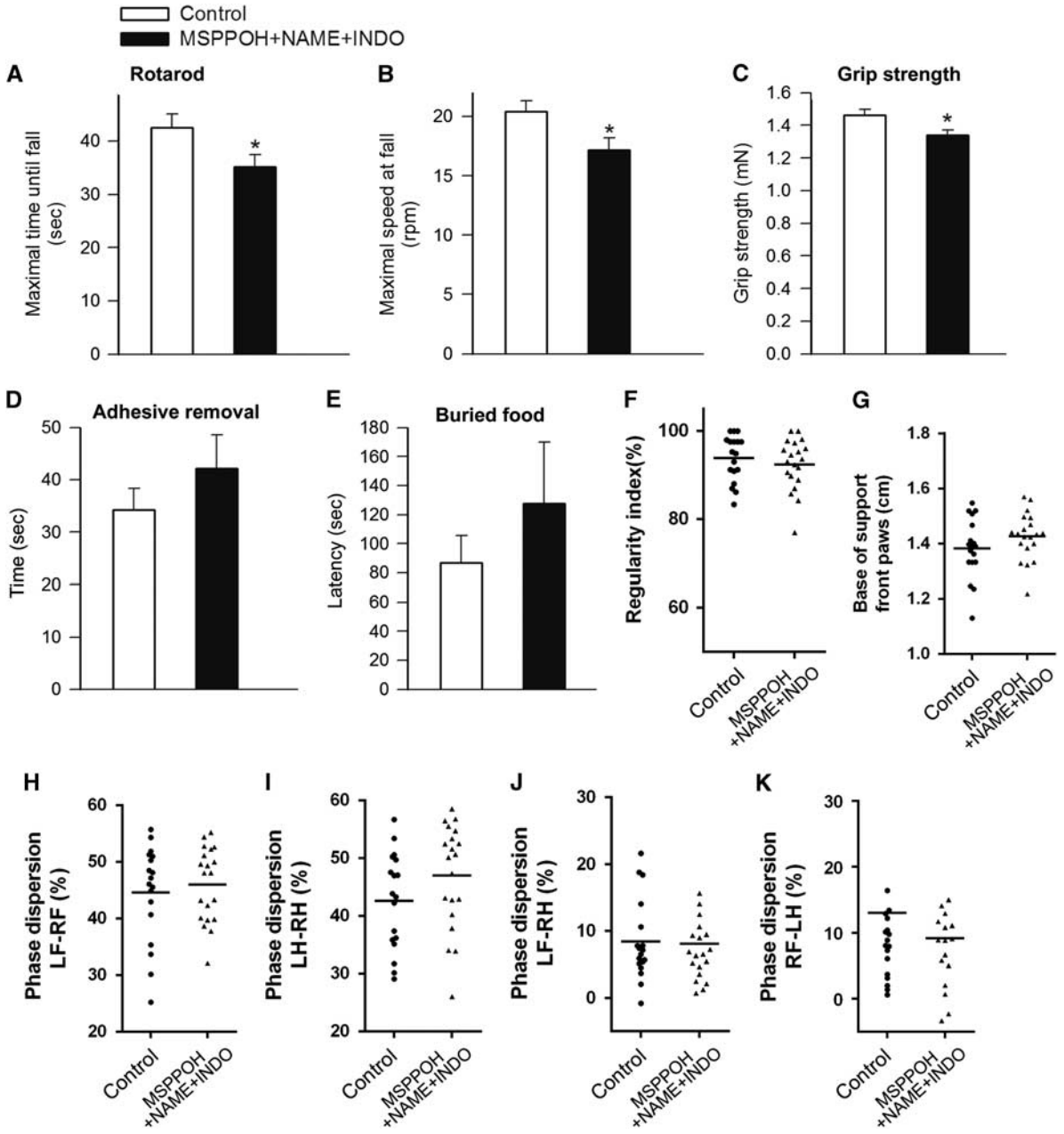

Figure 3. Effects of neurovascular uncoupling on sensorimotor function. (**A** and **B**) Rotarod testing. Time to fall during the accelerating rotarod test (**A**) and maximal speed at fall (**B**) are shown. Mice treated with MSPPOH+NAME+INDO showed impaired performance (time to fall, $^*P = 0.031$ versus control; maximal speed at fall, $^*P = 0.021$ versus control). Data are mean ± s.e.m. ($n = 20$ in each group). (**C**) Grip test. Average grip force was significantly less in mice treated with MSPPOH+NAME+INDO as compared with control mice ($P = 0.01$ versus Control). Data are mean ± s.e.m. ($n = 20$ in each group). There were no significant differences between the time needed to remove the adhesive from the forepaw (**D**, $P = 0.3$ versus Control) or the time needed to retrieve buried food (**E**; $P = 0.4$ versus Control). Data are mean ± s.e.m. ($n = 20$ in each group). (**F**–**K**) Effects of neurovascular uncoupling on gait coordination. A similar sequence regularity index (**F**; $P = 0.43$ versus Control) reflects no change in step patterns. Treatment with MSPPOH+NAME+INDO did not affect base of support (**G**). Phase dispersions (**H**–**K**) are unaltered for both the diagonal and the girdle pairs, showing no change in interpaw coordination (LH, left hind limb; RH, right hind limb; LF, left forelimb; RF, right forelimb; $n = 20$ in each group). INDO, indomethacin; MSPPOH, *N*-(methylsulfonyl)-2-(2-propynyloxy)-benzenehexanamide; L-NAME, L-NG-Nitroarginine methyl ester.

NO in the microcirculation by promoting oxidative stress, uncoupling endothelial NO synthase, and by upregulating asymmetric dimethylarginine, an endogenous inhibitor of NO synthase. Aging itself was shown to cause neurovascular uncoupling, at least in part, by impairing NO mediation of the response.[23,31] Increased oxidative stress and endothelial dysfunction are also known to affect arachidonic acid metabolism, decreasing production of vasodilator prostaglandins and EETs, and upregulating production of vasoconstrictor metabolites of arachidonic acid, such as 20-hydroxyeicosatetraenoic acid. Impaired synthesis/release of vasodilator arachidonic acid metabolites have been implicated in neurovascular uncoupling associated with IGF-1 deficiency (Toth and Ungvari, unpublished data 2014) and cerebral ischemia, as well. All of the aforementioned pathophysiologic conditions are associated with cognitive decline in experimental animals and human patients. On the basis

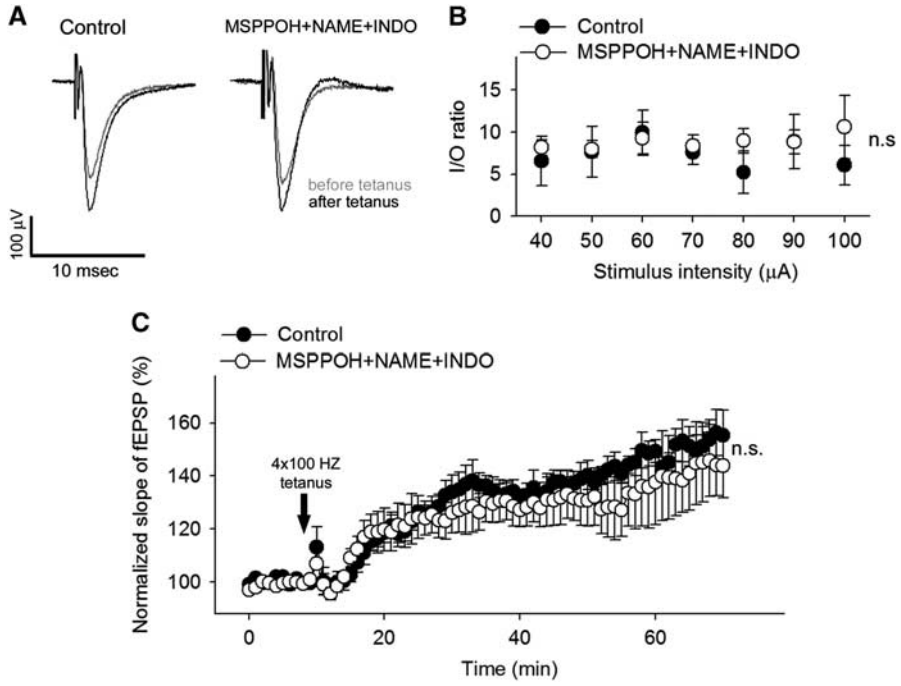

Figure 4. Treatment with MSPPOH+NAME+INDO does not affect synaptic function. (**A**) Original recordings showing the effects of treatment with MSPPOH+NAME+INDO on field excitatory postsynaptic potential (fEPSP) in the dentate gyrus in response to the stimulation of the perforant pathway (to 50 μA) on hippocampal brain slices before (10 minutes) and 1 hour after (70 minutes) 4 × 100 Hz tetanus. (**B**) Ratio of the evoked EPSP responses and the presynaptic fiber volley (I/O ratio) as a function of stimulus intensity in the dentate gyrus of hippocampal slices. Data are mean ± s.e.m. (control, $n = 11$; MSPPOH+NAME+INDO treated, $n = 7$; $P = 0.78$). (**C**) Long-term potentiation shown as change of fEPSP slope after a 4 × 100 Hz tetanic stimulus in the dentate gyrus of the hippocampus. Data are normalized to baseline responses and depicted as mean ± s.e.m. (control, $n = 11$; MSPPOH+NAME+INDO treated, $n = 7$; $P = 0.93$). INDO, indomethacin; MSPPOH, *N*-(methylsulfonyl)-2-(2-propynyloxy)-benzenehexanamide; L-NAME, L-NG-Nitroarginine methyl ester.

of our findings, we posit that therapeutic approaches that promote microvascular health and improve NVC should exert beneficial effects on cognitive function. Recent findings provide initial support for this concept showing that pharmacological interventions (e.g., treatment with resveratrol) that restore endothelial function and NVC[23] can improve cognitive function in aging.[41] Second, pharmacological treatments and dietary and lifestyle factors that interfere with synthesis of vasodilator NO, EETs, and prostaglandins impair NVC and thereby adversely affect cognitive function. For example, pharmacological inhibitors of the synthesis of vasodilator arachidonic acid metabolites were shown to impair NVC in humans.[38,42] The available data from the Baltimore Longitudinal Study on Aging also suggest that use of the cyclooxygenase inhibitor aspirin is associated with greater prospective cognitive decline.[43] Third, our findings provide strong evidence that neurovascular uncoupling induced by systemic influences and detected in the somatosensory cortex can predict impairment of cortical and hippocampal function. This result has important relevance for the interpretation of results from human studies, in which alterations of NVC are often characterized in the somatosensory cortex or in the primary visual cortex in the occipital lobe in response to visual stimuli.[42] Further studies are needed to provide direct evidence that findings obtained in the somatosensory cortex extend to other brain regions. The findings that experimentally-induced neurovascular uncoupling is also associated with sensorimotor deficits (Figure 3) warrant further studies investigating the role of impaired functional hyperemia in age-related slowing of sensorimotor processes. It is possible that functional consequences of neurovascular uncoupling show regional heterogeneity, which also should be elucidated by future investigations. There are excellent clinical studies, including the MOBILIZE Boston study,[35] linking neurovascular uncoupling to gait dysfunction. In the present study, experimentally-induced neurovascular uncoupling did not result in significant changes in the investigated indices of gait coordination (Figure 3). It is likely that the effects of acute neurovascular uncoupling on gait coordination in mice, if any, are subtle. Investigating gait variability, the stride-to-stride fluctuations in gait parameters, offers a more sensitive method of quantifying subtle changes in locomotion in mice, which should be considered in future studies. Finally, our results may also have important implications for functional brain imag fing in which functional hyperemia is commonly used as a surrogate for neural activation.

There is several line of evidence in support the concept that induction of neurovascular uncoupling is the main mechanism by which inhibition of synthesis of EETs, prostaglandins, and NO impairs cerebral function. Importantly, the pharmacological treatments employed did not affect evoked potential responses in the barrel cortex and basic synaptic transmission parameters and the normal long-term potentiation response of fEPSPs in the hippocampus (Figure 4). Previous studies also did not report significant changes in neuronal activity, including somatosensory evoked potentials, after pharmacologically-induced acute neurovascular uncoupling using inhibitors of NO synthesis, MSPPOH, and indomethacin.[37] It is also unlikely that impairment in learning and memory induced by short-term treatment with pharmacological inhibitors involves impaired neurogenesis.

Limitation of the Studies

We cannot exclude the possibility that the inhibition of synthesis of NO, prostaglandins, and EETs may also affect other aspects of neural, glial, or vascular mechanisms, which were not investigated in our studies. Although our studies show an association between

pharmacologically-induced neurovascular uncoupling and cognitive decline, further studies are needed to establish the cause and effect relationship.

Collectively, combined inhibition of synthesis of NO, EETs, and prostaglandins significantly reduces the blood flow responses to neuronal activation in the mouse brain, which mimics neurovascular uncoupling observed in aging and pathophysiologic conditions associated with accelerated cerebromicrovascular aging. The results of this study provide evidence that neurovascular uncoupling associates with cognitive decline. Our findings, taken together with the results of earlier studies, point to potential benefits of pharmacological and dietary interventions promoting microvascular health for prevention of cognitive decline.

AUTHOR CONTRIBUTIONS

ST, PH, ZT, AM, RT, EF, AC, WES, PT and ZU designed research and revised the manuscript; ST, PH, ZT, NMA, NS, EH, AM, PT, and AC performed experiments; ST, PH, AC, RT, NS, ZU, and PT analyzed data; ST, AC, PT, and ZU wrote the manuscript.

DISCLOSURE/CONFLICT OF INTEREST

The authors declare no conflict of interest.

REFERENCES

1 Zlokovic BV. Neurovascular pathways to neurodegeneration in Alzheimer's disease and other disorders. *Nat Rev Neurosci* 2011; **12**: 723–738.
2 Attwell D, Buchan AM, Charpak S, Lauritzen M, Macvicar BA, Newman EA. Glial and neuronal control of brain blood flow. *Nature* 2010; **468**: 232–243.
3 Ma J, Ayata C, Huang PL, Fishman MC, Moskowitz MA. Regional cerebral blood flow response to vibrissal stimulation in mice lacking type I NOS gene expression. *Am J Physiol* 1996; **270**: H1085–H1090.
4 Chen BR, Kozberg MG, Bouchard MB, Shaik MA, Hillman EM. A critical role for the vascular endothelium in functional neurovascular coupling in the brain. *J Am Heart Assoc* 2014; **3**: e000787.
5 Stobart JL, Lu L, Anderson HD, Mori H, Anderson CM. Astrocyte-induced cortical vasodilation is mediated by D-serine and endothelial nitric oxide synthase. *Proc Natl Acad Sci USA* 2013; **110**: 3149–3154.
6 Peng X, Carhuapoma JR, Bhardwaj A, Alkayed NJ, Falck JR, Harder DR *et al.* Suppression of cortical functional hyperemia to vibrissal stimulation in the rat by epoxygenase inhibitors. *Am J Physiol Heart Circ Physiol* 2002; **283**: H2029–H2037.
7 Takano T, Tian GF, Peng W, Lou N, Libionka W, Han X *et al.* Astrocyte-mediated control of cerebral blood flow. *Nat Neurosci* 2006; **9**: 260–267.
8 Zonta M, Angulo MC, Gobbo S, Rosengarten B, Hossmann KA, Pozzan T *et al.* Neuron-to-astrocyte signaling is central to the dynamic control of brain microcirculation. *Nat Neurosci* 2003; **6**: 43–50.
9 Stefanova I, Stephan T, Becker-Bense S, Dera T, Brandt T, Dieterich M. Age-related changes of blood-oxygen-level-dependent signal dynamics during optokinetic stimulation. *Neurobiol Aging* 2013; **34**: 2277–2286.
10 Topcuoglu MA, Aydin H, Saka E. Occipital cortex activation studied with simultaneous recordings of functional transcranial Doppler ultrasound (fTCD) and visual evoked potential (VEP) in cognitively normal human subjects: effect of healthy aging. *Neurosci Lett* 2009; **452**: 17–22.
11 Toth P, Tarantini S, Tucsek Z, Ashpole NM, Sosnowska D, Gautam T *et al.* Resveratrol treatment rescues neurovascular coupling in aged mice: role of improved cerebromicrovascular endothelial function and downregulation of NADPH oxidase. *Am J Physiol Heart Circ Physiol* 2014; **306**: H299–H308.
12 Kazama K, Anrather J, Zhou P, Girouard H, Frys K, Milner TA *et al.* Angiotensin II impairs neurovascular coupling in neocortex through NADPH oxidase-derived radicals. *Circ Res* 2004; **95**: 1019–1026.
13 Tucsek Z, Toth P, Sosnowska D, Gautam T, Mitschelen M, Koller A *et al.* Obesity in aging exacerbates blood-brain barrier disruption, neuroinflammation, and oxidative stress in the mouse hippocampus: effects on expression of genes involved in beta-amyloid generation and Alzheimer's disease. *J Gerontol A Biol Sci Med Sci* 2013; **69**: 1212–1226.
14 Girouard H, Iadecola C. Neurovascular coupling in the normal brain and in hypertension, stroke, and Alzheimer disease. *J Appl Physiol* 2006; **100**: 328–335.
15 Heinzel S, Liepelt-Scarfone I, Roeben B, Nasi-Kordhishti I, Suenkel U, Wurster I *et al.* A neurodegenerative vascular burden index and the impact on cognition. *Front Aging Neurosci* 2014; **6**: 161.
16 Brand-Schieber E, Falck JF, Schwartzman M. Selective inhibition of arachidonic acid epoxidation in vivo. *J Physiol Pharmacol* 2000; **51**: 655–672.
17 Wakisaka Y, Chu Y, Miller JD, Rosenberg GA, Heistad DD. Spontaneous intracerebral hemorrhage during acute and chronic hypertension in mice. *J Cereb Blood Flow Metab* 2010; **30**: 56–69.
18 Toth P, Tucsek Z, Sosnowska D, Gautam T, Mitschelen M, Tarantini S *et al.* Age-related autoregulatory dysfunction and cerebromicrovascular injury in mice with angiotensin II-induced hypertension. *J Cereb Blood Flow Metab* 2013; **33**: 1732–1742.
19 Antunes M, Biala G. The novel object recognition memory: neurobiology, test procedure, and its modifications. *Cogn Process* 2012; **13**: 93–110.
20 MacLaren DA, Santini JA, Russell AL, Markovic T, Clark SD. Deficits in motor performance after pedunculopontine lesions in rats—impairment depends on demands of task. *Eur J Neurosci* 2014; **40**: 3224–3236.
21 Bouet V, Boulouard M, Toutain J, Divoux D, Bernaudin M, Schumann-Bard P *et al.* The adhesive removal test: a sensitive method to assess sensorimotor deficits in mice. *Nat Protoc* 2009; **4**: 1560–1564.
22 Hamers FP, Koopmans GC, Joosten EA. CatWalk-assisted gait analysis in the assessment of spinal cord injury. *J Neurotrauma* 2006; **23**: 537–548.
23 Toth P, Tarantini S, Tucsek Z, Ashpole NM, Sosnowska D, Gautam T *et al.* Resveratrol treatment rescues neurovascular coupling in aged mice:role of improved cerebromicrovascular endothelial function and down-regulation of NADPH oxidase. *Am J Physiol Heart Circ Physiol* 2014; **306**: H299–H308.
24 Lind BL, Brazhe AR, Jessen SB, Tan FC, Lauritzen MJ. Rapid stimulus-evoked astrocyte Ca2+ elevations and hemodynamic responses in mouse somatosensory cortex in vivo. *Proc Natl Acad Sci USA* 2013; **110**: E4678–E4687.
25 Nehlig A, Wittendorp-Rechenmann E, Lam CD. Selective uptake of [14C]2-deoxyglucose by neurons and astrocytes: high-resolution microautoradiographic imaging by cellular 14C-trajectography combined with immunohistochemistry. *J Cereb Blood Flow Metab* 2004; **24**: 1004–1014.
26 Frayling C, Britton R, Dale N. ATP-mediated glucosensing by hypothalamic tanycytes. *J Physiol* 2011; **589**: 2275–2286.
27 Leithner C, Muller S, Fuchtemeier M, Lindauer U, Dirnagl U, Royl G. Determination of the brain-blood partition coefficient for water in mice using MRI. *J Cereb Blood Flow Metab* 2010; **30**: 1821–1824.
28 Garteiser P, Doblas S, Watanabe Y, Saunders D, Hoyle J, Lerner M *et al.* Multiparametric assessment of the anti-glioma properties of OKN007 by magnetic resonance imaging. *J Magn Reson Imaging* 2010; **31**: 796–806.
29 Herscovitch P, Raichle ME. What is the correct value for the brain--blood partition coefficient for water? *J Cereb Blood Flow Metab* 1985; **5**: 65–69.
30 Oka H, Shimono K, Ogawa R, Sugihara H, Taketani M. A new planar multielectrode array for extracellular recording: application to hippocampal acute slice. *J Neurosci Methods* 1999; **93**: 61–67.
31 Park L, Anrather J, Girouard H, Zhou P, Iadecola C. Nox2-derived reactive oxygen species mediate neurovascular dysregulation in the aging mouse brain. *J Cereb Blood Flow Metab* 2007; **27**: 1908–1918.
32 Keisker B, Hepp-Reymond MC, Blickenstorfer A, Kollias SS. Differential representation of dynamic and static power grip force in the sensorimotor network. *Eur J Neurosci* 2010; **31**: 1483–1491.
33 Stenholm S, Sallinen J, Koster A, Rantanen T, Sainio P, Heliövaara M *et al.* Association between obesity history and hand grip strength in older adults--exploring the roles of inflammation and insulin resistance as mediating factors. *J Gerontol A Biol Sci Med Sci* 2011; **66**: 341–348.
34 Petzold GC, Albeanu DF, Sato TF, Murthy VN. Coupling of neural activity to blood flow in olfactory glomeruli is mediated by astrocytic pathways. *Neuron* 2008; **58**: 897–910.
35 Sorond FA, Kiely DK, Galica A, Moscufo N, Serrador JM, Iloputaife I *et al.* Neurovascular coupling is impaired in slow walkers: the MOBILIZE Boston Study. *Ann Neurol* 2011; **70**: 213–220.
36 Gorelick PB, Scuteri A, Black SE, Decarli C, Greenberg SM, Iadecola C *et al.* Vascular contributions to cognitive impairment and dementia: a statement for healthcare professionals from the american heart association/american stroke association. *Stroke* 2011; **42**: 2672–2713.
37 Leithner C, Royl G, Offenhauser N, Füchtemeier M, Kohl-Bareis M, Villringer A *et al.* Pharmacological uncoupling of activation induced increases in CBF and CMRO2. *J Cereb Blood Flow Metab* 2010; **30**: 311–322.
38 Bruhn H, Fransson P, Frahm J. Modulation of cerebral blood oxygenation by indomethacin: MRI at rest and functional brain activation. *J Magn Reson Imaging* 2001; **13**: 325–334.
39 Mitschelen M, Garteiser P, Carnes BA, Farley JA, Doblas S, Demoe JH *et al.* Basal and hypercapnia-altered cerebrovascular perfusion predict mild cognitive impairment in aging rodents. *Neuroscience* 2009; **164**: 918–928.

40 Miralbell J, Lopez-Cancio E, Lopez-Oloriz J, Arenillas JF, Barrios M, Soriano-Raya JJ *et al*. Cognitive patterns in relation to biomarkers of cerebrovascular disease and vascular risk factors. *Cerebrovasc Dis* 2013; **36**: 98–105.

41 Witte AV, Kerti L, Margulies DS, Floel A. Effects of resveratrol on memory performance, hippocampal functional connectivity, and glucose metabolism in healthy older adults. *J Neurosci* 2014; **34**: 7862–7870.

42 Szabo K, Rosengarten B, Juhasz T, Lako E, Csiba L, Olah L. Effect of non-steroid anti-inflammatory drugs on neurovascular coupling in humans. *J Neurol Sci* 2014; **336**: 227–231.

43 Waldstein SR, Wendell CR, Seliger SL, Ferrucci L, Metter EJ, Zonderman AB. Nonsteroidal anti-inflammatory drugs, aspirin, and cognitive function in the Baltimore longitudinal study of aging. *J Am Geriatr Soc* 2010; **58**: 38–43.